Isolation and Structure Assignments of Rostratins A−D, Cytotoxic Disulfides Produced by the Marine-Derived Fungus *Exserohilum rostratum*†

Ren Xiang Tan,‡ Paul R. Jensen,§ Philip G. Williams,§ and William Fenical*,§

Center for Marine Biotechnology and Biomedicine, Scripps Institution of Oceanography, University of California, San Diego, La Jolla, California 92093-0204

Received February 18, 2004

Four new cytotoxic disulfides, rostratins A−D (**1**−**4**), were isolated from the whole broth of the marine-derived fungus *Exserohilum rostratum* (Drechsler), a fungal strain found associated with a marine cyanobacterial mat. The structures of these cyclic dipeptides were established through chemical degradation and a variety of two-dimensional NMR techniques. The absolute configurations of the rostratins were determined by the modified Mosher method. In the case of the polyhydroxylated compound **1** and the mercaptol **4**, regioselective acylation was achieved by modulating the reaction temperature while monitoring the progress of the reaction by ^{1}H NMR. Rostratins A, B, C, and D showed in vitro cytotoxicity against human colon carcinoma (HCT-116) with IC_{50} values of 8.5, 1.9, 0.76, and 16.5 μg/mL, respectively.

Although cancer continues to be one of the most difficult life-threatening diseases to treat, drugs derived from natural products have helped to ameliorate the situation.[1] Of the natural products available, those from marine organisms have proven to be an excellent source of new lead compounds, with over 15 drugs derived from marine natural products currently in human clinical trials.[2] Developing marine-derived drugs has been difficult however, since the supply of these new molecules is often limited by the difficulty in large-scale re-collecting and because marine invertebrates are not easily cultured.[2] More recently, we and others began to explore marine microbes as a source of new drug leads because they allow for the scale-up of production and thus avoid many of the challenges associated with harvesting invertebrates. Furthermore, the chemical diversity of marine microbial secondary metabolites reported to date has shown that these are excellent resources for the discovery of new drugs.[2,3] Even though our understanding of marine microbial biodiversity has been based on limited studies of diverse ocean environments, the microorganisms isolated have produced a broad range of chemically novel and biologically active secondary metabolites.[2,4]

Results and Discussion

As a continuation of our previous investigations aimed at characterizing new secondary metabolites that inhibit cancer cells,[5−7] we found that the ethyl acetate extract of the whole culture of fungal strain CNK-630 showed pronounced in vitro cytotoxicity against the human colon carcinoma cell line HCT-116. This marine-derived fungal strain was found associated with a cyanobacterial mat collected off the island of Lanai, Hawaii, in 1997, and was subsequently identified as *Exserohilum rostratum*, a terrestrial plant pathogen that has also been recovered from mangrove leaves[8] and used as a biocontrol agent.[9] Thus, *E. rostratum* joins the ranks of fungal species that can be isolated from both marine and terrestrial sources. Although it is not certain what percentage of these fungal species are able to grow and reproduce in the marine environment, some of these species have been shown to play important ecological roles, e.g., as marine invertebrate pathogens.[10] This suggests that they are not merely terrestrial contaminants present in the marine environment as dormant spores.

Using bioassay-guided fractionation[11] of the whole culture extract, four new highly symmetrical cytotoxic diketopiperazine disulfides, rostratins A−D (**1**−**4**), were isolated along with the known compound exserohilone (**5**), a phytotoxin reported earlier from the terrestrial fungus *Exserohilum holmii*.[12] In this paper, we report the isolation of these compounds, their structure determinations involving chemical degradation and spectral analyses, and their bioactivities against cancer cells. Also in this report, we describe a new method for selective monoacylation [using 2-methoxy-2-(trifluoromethyl)phenylacetyl chloride in pyridine] of polyfunctional metabolites using a temperature-modulated, in-NMR-tube, acylation method. This technique is demonstrated in the selective acylation of **1** and **4** to produce the corresponding mono-(bis)-(*R*)- and (*S*)-MTPA esters, thus facilitating the confident determination of the absolute stereochemistries for these metabolites.

Rostratin A (**1**) was isolated as an optically active colorless gum, which had strong IR absorption bands at 3331 and 1666 cm^{-1} indicative of hydroxyl and amide functional groups. The low-resolution ESI mass spectrum of compound **1** showed an intense $[M + H]^+$ pseudomolecular ion at *m*/*z* 429 (positive mode) and a prominent $[M + {}^{35}Cl]^-$ ion at *m*/*z* 463 in the negative mode. High-resolution MALDI mass spectral data showed a pronounced fragment ion at *m*/*z* 365.1723 ($[C_{18}H_{24}N_2O_6 + H]^+$ requires 365.1713) produced through elimination of S_2 from the protonated molecular ion of **1**. These combined mass spectral data allowed the molecular formula of **1** to be assigned as $C_{18}H_{24}N_2O_6S_2$.

The overall NMR spectral data for rostratin A (**1**), which included results from COSY and spin decoupling experiments, showed the presence of a complex 10-proton spin system that defined a major portion of the molecule (see

† Dedicated to the late Dr. D. John Faulkner (Scripps) and the late Dr. Paul J. Scheuer (Hawaii) for their pioneering work on bioactive marine natural products.

* To whom correspondence should be addressed. Tel: (858) 534-2133. Fax: (858) 558-3702. E-mail: wfenical@ucsd.edu.

‡ On sabbatical leave from the Institute of Functional Biomolecules, Nanjing University, Nanjing, People's Republic of China.

§ Scripps Institution of Oceanography.

10.1021/np049920b CCC: $27.50
Published on Web 07/10/2004

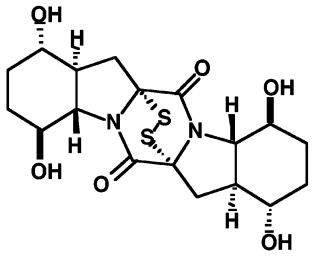

1, rostratin A

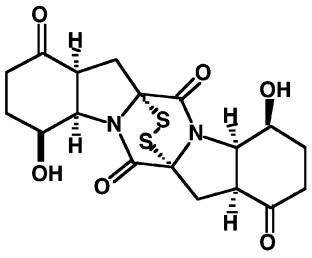

2, rostratin B

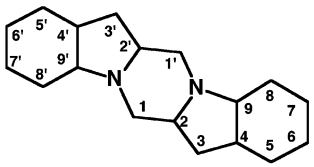

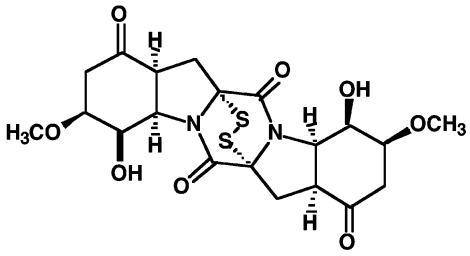

3, rostratin C

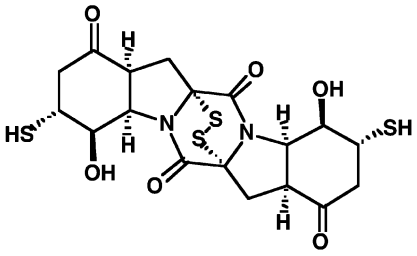

4, rostratin D

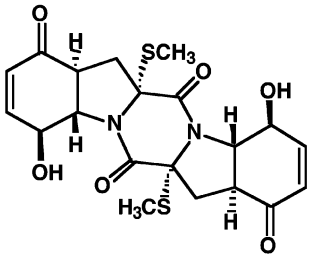

5, exserohilone

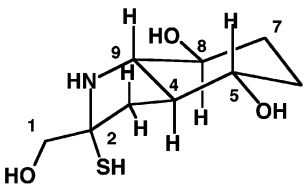

6

Table 1). This spin system was comprised of a methylene pair observed at δ 2.59 (J = 14.4, 12.2 Hz) and 2.41 (J = 14.4, 5.2 Hz) that was coupled to a methine proton at δ 2.09 (J = 12.2, 12.0, 11.7, 5.2 Hz), which was itself coupled to a methine proton at δ 3.52 (dddd, J = 11.7, 10.7, 5.2, 4.8 Hz). This latter methine was coupled to a diastereotopic methylene pair (δ 1.30 and 1.85) that were coupled to a second methylene pair at δ 1.95 and 1.26. This latter methylene pair was further coupled to a methine proton (δ 3.64, ddd, J = 12.5, 10.5, 5.8 Hz) that was further coupled to another methine proton at δ 3.41 (J = 12.0, 10.5 Hz). COSY data further showed that this latter methine proton was coupled to the δ 2.09 multiplet, thus indicating the presence of a six-membered carbon ring (later assigned to the C-3(3′) to C-9(9′) cyclohexane system).

The ^{13}C NMR spectrum of **1**, including DEPT sequence data, showed a total of nine resonance lines consisting of three methylene, four methine (three oxygenated carbons at δ 70.7, 70.0, and 69.0), and two quaternary carbons (δ 164.7 and 75.9). These ^{1}H and ^{13}C NMR data accounted for only half of the carbon and hydrogen composition given by the molecular formula. The amide carbonyl signal at δ 164.7, coupled with the molecular formula and the simultaneous isolation of **5**, suggested that **1** was most probably a cyclic dipeptide (a diketopiperazine) composed of α-substituted α-amino acids.[13,14] This observation, along with the IR amide absorption bands at 1666 cm^{-1}, demonstrated that compound **1** was a symmetrical diketopiperazine related to exserohilone (**5**), which are the dimerization products of highly oxidized phenylalanine residues.[12]

The unambiguous assignment of all ^{1}H and ^{13}C NMR signals for rostratin A (**1**) was achieved by analysis of COSY, HMQC, NOESY, and HMBC spectral data (Table 1). In the HMBC spectrum of **1**, the two quaternary carbon signals at δ 164.7 (C-1/1′) and 75.9 (C-2/2′) correlated with the diastereotopic methylene protons at δ 2.41 (H-3/3′) and 2.59 (H-3/3′), both of which showed additional correlations with the methine carbon signals at δ 48.3 (C-4/4′), 69.0 (C-5/5′), and 70.7 (C-9/9′). Furthermore, both the C-4(4′) and C-9(9′) carbon signals yielded HMBC correlations to H-5(5′) and H-8(8′) protons, which also correlated with the two methylene carbons at δ 33.1 (C-6/6′) and 31.0 (C-7/7′). These overall data defined a phenylalanine-derived diketopiperazine dimer formed by oxidation of the aromatic ring in the C-5(5′) and C-8(8′) positions. Consistent with the bismethyl sulfide substitution pattern of exserohilone (**5**), the disulfide bridge in **1** was positioned between carbons C-2 and C-2′.

The relative stereochemistry of rostratin A was suspected to be identical to that of exserohilone, the structure of which was secured by X-ray analysis.[12] This assumption was confirmed by comprehensive chemical shift and coupling constant analysis, which defined the positions of all substituents, and application of the classic Karplus Equation to define the conformation of the substituents on the cyclohexane ring. The ring juncture protons H-4(4′) and H-9(9′) both showed a large vicinal coupling constant (11.7 Hz) consistent with a *trans*-diaxial ring juncture. Using this as a starting point, the remaining relative stereochemistry of **1** was established using NOE difference and NOESY spectral data (see Figure 1). From NOE data, H-9(9′) showed NOE correlations with the downfield H-3(3′) signal, H-5(5′), and H-7β(7′β), demonstrating that these three protons were spatially arranged on the top face of the molecule (all axial protons). As expected, NOE correlations were not observed between H-9(9′) and H-4(4′); instead, H-4(4′) showed a clear NOE correlation with H-8(8′), indicating these protons were in axial positions on the bottom face of the molecule. Since H-5(5′) and H-8(8′) had both been defined as axial, the hydroxyl groups at these carbons were assigned equatorial positions.

Next, we considered several alternatives to determine the absolute stereochemistry of rostratin A. Spectral methods such as exciton coupling,[15] X-ray crystallography, and NMR strategies such as the commonly utilized modified Mosher's methods[16,17] are often the techniques of choice. The Mosher (modified) method, involving the independent esterification of a secondary alcohol or amine with (*S*)- and (*R*)-2-methoxy-2-(trifluoromethyl)phenylacetyl chlorides (MTPA-Cl) and analysis of the chemical shift data

Table 1. NMR Spectral Assignments for **1** in DMSO-d_6

C#	δ_C	δ_H (m, *J* in Hz)	COSY	HMBC
1/1′	164.7, C			3/3′
2/2′	75.9, C			3/3′
3/3′	33.9, CH2	(α) 2.41 (dd, 14.4, 5.2)	3/3′(β), 4/4′	4/4′
		(β) 2.59 (dd, 14.4, 12.2)	3/3′(α), 4/4′	
4/4′	48.3, CH	2.09 (dddd, 12.2, 12.0, 11.7, 5.2)	3/3′, 5/5′, 9/9′	5/5′-OH, 8/8′, 5/5′, 9/9′, 3/3′(β), 6/6′(β)
5/5′	69.0, CH	3.52 (dddd, 11.7, 10.7, 5.2, 4.8)	5/5′-OH, 6/6′	5/5′-OH, 9/9′, 3/3′(β), 7/7′(β)
6/6′	33.1, CH2	(α) 1.30 (m)	5/5′, 6/6′(β), 7/7′	4/4′, 5/5′-OH
		(β) 1.85 (m)	5/5′, 6/6′(α), 7/7′	
7/7′	31.0, CH2	(α) 1.95 (m)	6/6′, 7/7′(β), 8/8′	8/8′-OH, 9/9′
		(β) 1.26 (m)	7/7′(α), 6/6′, 8/8′	
8/8′	70.0, CH	3.64 (ddd, 12.5, 10.5, 5.8)	4/4′, 7/7′	6/6′(α), 8/8′-OH, 9/9′
9/9′	70.7, CH	3.41 (dd, 12.0, 10.5)	4/4′, 8/8′	3/3′(α), 5/5′, 8/8′
5/5′-OH		5.08 (d, 4.8)	5/5′	
8/8′-OH		6.08 (s)		

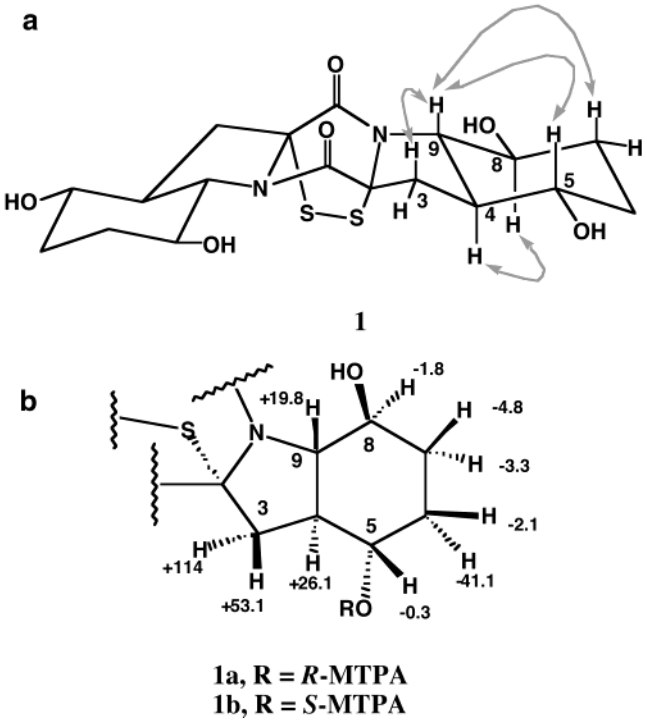

1

1a, R = *R*-MTPA
1b, R = *S*-MTPA

Figure 1. Relative and absolute stereochemistry of rostratin A (**1**): (a) arrows indicate critical NOE correlations used to establish relative stereochemistry and (b) $\Delta\delta$ values ($\delta_S - \delta_R$) in hertz for the two MTPA esters **1a** and **1b**.

from the corresponding esters, has been most frequently utilized.[17] Application of this method generally requires that the (*S*)- and (*R*)-MTPA esters be isolated and purified and that assignable ^{1}H NMR chemical shift data be recorded from each sample. This prerequisite often poses great difficulties when dealing with small amounts of compounds, a situation frequently faced with natural products. Recent innovations such as LC-NMR analyses of Mosher esters immediately after acylation[18] and in-NMR-tube measurements[19] have improved this situation, but only when clear shift data are generated from mono MTPA esters. The inherent difficulty in interpreting the complex chemical shifts observed for the multiple MTPA esters produced from polyhydroxylated/multifunctional compounds has rendered this method of limited use.[20] By careful analyses of the chemical shift data from 1,3-diol and 1,3,5-triol MTPA esters, it has been possible to make confident assignments.[21−23]

Because of these problems with polyhydroxylated compounds, it has often been necessary to undertake selective protection steps in order to generate a monofunctional molecule prior to MTPA acylation.[7] This approach has been successful in several cases, but is often impossible due to the lack of protecting group selectivity and sample size limitations.

To solve the absolute stereochemistry of rostratin A, we considered ways to regioselectively acylate **1** to produce a mono (bis) MTPA ester. The solution to this problem was the development of the selective Mosher reaction, an in-NMR-tube method that capitalizes on the differential rates of acylation at reduced temperatures. Using simple temperature control of the acylation reaction (MTPA-Cl/pyridine) performed in the NMR tube, we were able to regioselectively acylate the C-5(5′) hydroxyl group in **1**.

Initial inspection of the molecular model of rostratin A (**1**) showed that both equatorial hydroxyls in the cyclohexane-1,4-diol have similar spatial accessibility. Thus, the formation of multiple MTPA esters, in which the proton chemical shifts would be difficult if not impossible to interpret,[13,14] seemed inevitable if the standard procedure for MTPA acylation was followed.[16] To affect selective monoacylation of one of the two (symmetrical) secondary hydroxyls in the cyclohexane-1,4-diol moiety, compound **1** was dissolved in pyridine-d_5 in an NMR tube dried under a nitrogen stream, and a baseline ^{1}H NMR spectrum was acquired (see Supporting Information, Figure S1a). The lower half of the NMR tube was maintained at approximately −5 °C using a salt−ice bath, and after 10 min 2.4 molar equiv of (*R*)-MTPA chloride was added. The tube was shaken to afford even mixing and maintained at −5 °C for 1 h, during which spectra were recorded every 30 min to monitor the rate of acylation. The NMR tube was then slowly warmed from −5 to 28 °C at the rate of 1 °C every 5 min. At 28 °C, acylation of the C-5(5′) hydroxyl began; thus this reaction temperature was maintained for another 3 h until the reaction had gone to completion (Figure S1b).[24] Excess (*R*)-MTPA chloride was destroyed by adding a drop of D_2O, and COSY NMR data of the resulting (*S*)-MTPA ester (**1b**) were recorded (Figure S2), confirming that selective acylation had occurred exclusively at the C-5(5′)-hydroxyl position. Similarly, compound **1** was selectively acylated at C-5(5′) with (*S*)-MTPA-Cl to generate the (*R*)-MTPA ester **1a**, the ^{1}H NMR spectrum of which is shown in Figure S1c.

Analysis of the proton chemical shift $\Delta\delta$ values between the (*S*)- and (*R*)-MTPA esters demonstrated that C-5(5′) has the *S*-configuration [$\Delta\delta$ values (= $\delta_S - \delta_R$) in Hz are given in Figure 1]. This information, along with the aforementioned NOESY data, defined the absolute configurations at C-4(4′), C-8(8′), and C-9(9′) in rostratin A as *S*, *S*, and *S*, respectively.

One of the difficulties in employing in-NMR-tube acylations is recognizing individual proton chemical shifts of esters in complex reaction mixtures. Indeed Su et al.[19] have

Table 2. NMR Spectral Assignments for **2** in DMSO-d_6

C#	δ_C	δ_H (m, *J* in Hz)	COSY	HMBC
1/1′	162.0, C			3/3′(β)
2/2′	76.2, C			4/4′, 3/3′
3/3′	32.2, CH2	(α) 2.72 (dd, 14.8, 1.6)	3/3′(β), 4/4′	4/4′
		(β) 2.92 (dd, 14.8, 8.4)	3/3′(α), 4/4′	
4/4′	46.7, CH	3.21 (br dd, 8.4, 7.2)	3/3′, 8/8′	3/3′
5/5′	208.3, C			9/9′, 4/4′, 3/3′, 6/6′, 7/7′(β)
6/6′	33.9, CH2	(α) 2.26 (ddd, 16.4, 4.4, 3.6)	6/6′(β), 7/7′	4/4′
		(β) 2.67 (ddd, 16.4, 12.6, 6.0)	6/6′(α), 7/7′	
7/7′	25.4, CH2	(α) 1.62 (br ddd, 12.6, 12.3, 4.4)	6/6′, 7/7′(β), 8/8′	OH, 9/9′, 6/6′(β)
		(β) 1.87 (m)	6/6′, 7/7′(α), 8/8′	
8/8′	60.7, CH	4.81 (m)	OH, 7/7′, 9/9′	OH, 9/9′, 6/6′(β)
9/9′	65.6, CH	4.35 (dd, 7.2, 3.2)	4/4′, 8/8′	OH, 4/4′, 3/3′(α)
OH		5.47 (d, 3.6)	8/8′	

commented on the difficulty in recording chemical shifts in the presence of MTPA-related byproducts. We observed this complexity in measuring the shifts of ester **1a**, in which the H-9(9′) signal was partially obscured by an impurity methoxy singlet originating from an (*S*)-MTPA-Cl-related byproduct. We found the application of NOE difference spectroscopy to be an efficient technique for tackling the overlap issue. Although obscured, the H-9(9′) proton signal was selectively visualized at δ 3.65 (dd, J = 10.8, 8.7 Hz), independent of all other signals, by measurement of the NOE difference spectrum upon irradiation of the H-5(5′) signal at δ 5.32 (Figure S1d).

In rostratin A (**1**), neither the relative nor absolute configuration of the C-2(2′) disulfide bridge carbons could be directly established by spectroscopic methods. Even though metabolite **1** most probably shares the same C-2(2′) stereochemistry as exserohilone (**5**), whose relative configuration was established by X-ray crystallographic analysis of its *p*-bromobenzoate derivative,[12] the assignment could not be made with confidence. To establish the stereochemistry at these centers, metabolite **1** was reduced with $LiAlH_4$ to yield the amino alcohol **6**.[25] By taking advantage of the protons of the newly formed 1° alcohol group in **6**, the C-2 (thiol bearing) configuration could be defined. As anticipated, all ^{1}H NMR signals of **6**, and the stereochemistry of the compound, could be assigned by ^{1}H NMR COSY and NOESY spectral methods, along with spin decoupling and NOE difference experiments. The hydroxymethyl protons (H_2-1), which appeared at δ 3.72, showed clear NOE correlations with H-3α (δ 1.39) and H-3β (δ 2.01), the latter of which showed an NOE correlation with H-9 (δ 3.68), confirming the locations of these protons on the top face of the molecule. These data showed that the hydroxymethyl group was equatorial and the thiol functional group was oriented in an axial position. Translation of the stereochemistry of **6** to metabolite **1** allowed the absolute stereochemistry at C-2(2′) to be assigned as *R*. These combined spectral and chemical studies fully defined rostratin A as the new disulfide diketopiperazine **1**.

Rostratin B (**2**) was obtained as a colorless gum, which displayed strong IR absorption bands at 3413 (OH), 1705 (ketone), and 1666 (amide) cm^{-1}. The positive mode API-ES mass spectrum of **2** showed an $[M + H]^+$ peak at *m/z* 425, while in the negative mode an intense $[M + {}^{35}Cl]^-$ pseudo molecular ion was observed at *m/z* 459. As in **1**, the high-resolution MALDI mass spectrum showed an abundant fragment ion at *m/z* 361.1387 ($[C_{18}H_{20}N_2O_6 + H]^+$ requires 361.1400) produced through the loss of S_2 from the protonated molecular ion. These combined mass spectral data showed the molecular formula for **2** to be $C_{18}H_{20}N_2O_6S_2$, a molecular formula possessing an extra two degrees of unsaturation in comparison to rostratin A (**1**).

The combined NMR spectral features of **2** were similar to those of rostratin A, but proton coupling constant data immediately showed that **2** was configurationally different than **1**. Analysis of ^{1}H NMR data (Table 2) showed that the cyclohexane rings were intact. However, analysis of the proton−proton coupling constants indicated that the C-4(4′)−C-9(9′) ring juncture was most likely *cis* ($J_{H-4/H-9}$ = 7.2 Hz) in **2**, in comparison with the *trans* configuration in **1** ($J_{H-4/H-9}$ = 11.7 Hz). NMR data further showed that the hydroxyl functionalities at C-5(5′) in **1** were absent. IR absorption characteristics of a ketone functional group and a characteristic six-proton spin system from C-6(6′) to C-9(9′) showed that rostratin B possessed ketone functional groups at C-5(5′) (δ 208.3). As in **1**, the overall NMR features showed that **2** was a symmetrical molecule with only half of the proton and carbon bands being observed. Furthermore, the carbon signal at δ 162.0 and an IR absorption band at 1666 cm^{-1} indicated that compound **2** was also a diketopiperazine, possibly with the same cyclic disulfide. This assumption was subsequently confirmed by comprehensive analysis of COSY, NOESY, HMQC, and HMBC data, which allowed the complete assignment of all ^{1}H and ^{13}C NMR signals (Table 2), confirming the structure assignment as shown in **2**.

The relative stereochemistry for **2**, including the C-4(4′)−C-9(9′) *cis* ring juncture, was confirmed by NOE difference spectroscopy (Figure 2). Irradiation of the H-9(9′) signal at δ 4.35 produced strong NOE enhancements of the H-4(4′) and H-8(8′) protons, indicating they are positioned in spatial proximity on the bottom face of the molecule. These enhancements showed that H-8(8′) was in an equatorial proton, hence indicating that the C-8(8′) hydroxyl functionalities were in axial positions. Irradiation of H-4(4′) also produced enhancements of the H-3α(3′α) proton signal, again positioned within NOE distance on the bottom face. Comprehensive analysis of molecular models of **2** and comparison with the measured vicinal coupling constant data showed that both cyclohexane rings were in chair conformations. These data confirmed the relative stereochemistry of rostratin B as shown in **2**.

The absolute stereochemistry of rostratin B (**2**) was determined by the modified Mosher method as described by Su and co-workers.[19] In separate in-NMR-tube reactions, (*S*)- and (*R*)-MTPA-Cl acylation of **2** yielded the corresponding C-8(8′) (*R*)- and (*S*)-MTPA bis-esters **2a** and **2b**, respectively. The striking difference in proton chemical shifts between these esters showed that C-8(8′) possesses the *S*-configuration ($\Delta\delta$ values = $\delta_S - \delta_R$ in Hz are given in Figure 2). Given the relative stereochemistry determined by NOE data, C-4(4′) and C-9(9′) can be assigned the *S*- and *R*-configurations, respectively. Although in **2** we did not rigorously prove the α-configuration of the disulfide

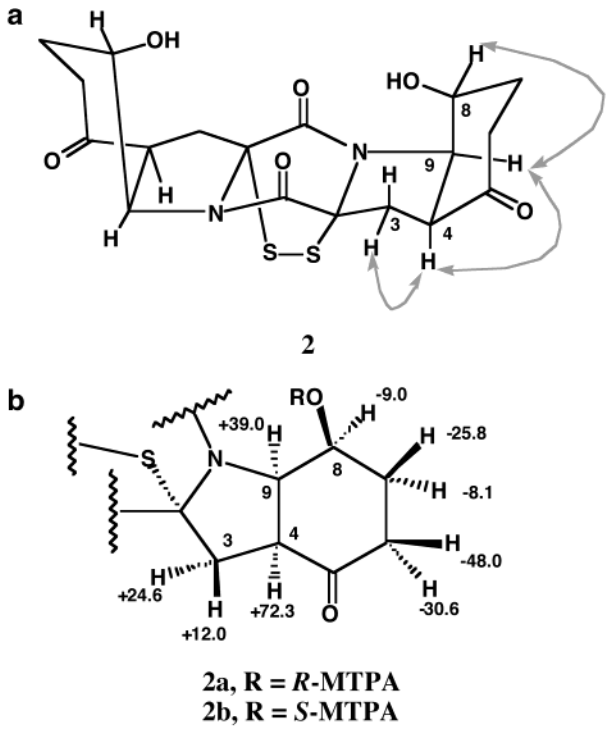

Figure 2. Relative and absolute stereochemistry of rostratin B (**2**): (a) arrows indicate critical NOE correlations used to establish relative stereochemistry and (b) $\Delta\delta$ values ($\delta_S - \delta_R$) in hertz for the two MTPA esters **2a** and **2b**.

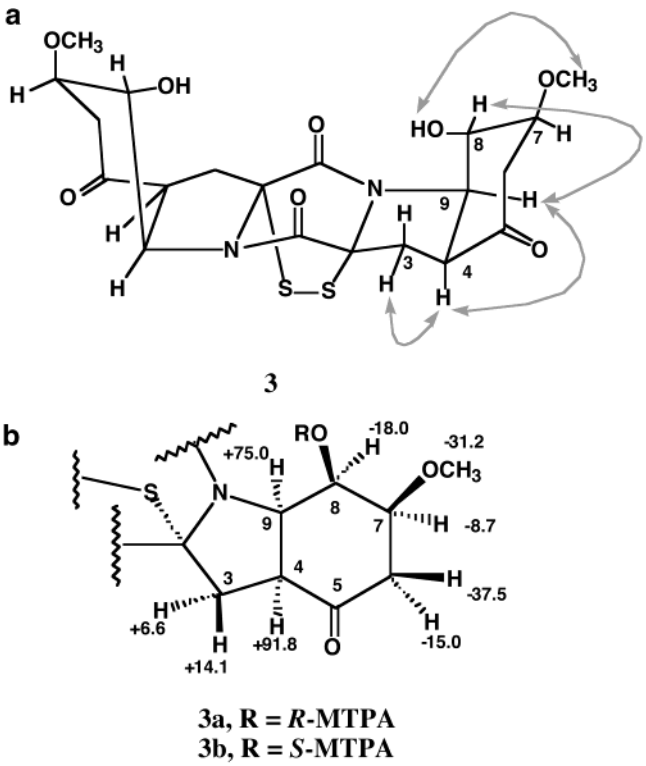

Figure 3. Relative and absolute stereochemistry of rostratin C (**3**): (a) arrows indicate critical NOE correlations used to establish relative stereochemistry and (b) $\Delta\delta$ values ($\delta_S - \delta_R$) in hertz for the two MTPA esters **3a** and **3b**.

bridge, the overall comparison of this metabolite to **1** strongly indicates the same diketopiperazine array.

Rostratin C (**3**) was also isolated as an optically active colorless gum, which showed strong IR absorptions at 3395 (OH), 1703 (ketone), and 1673 (amide) cm^{-1}. ESI mass spectral data showed an intense $[M + Na]^+$ peak at *m/z*

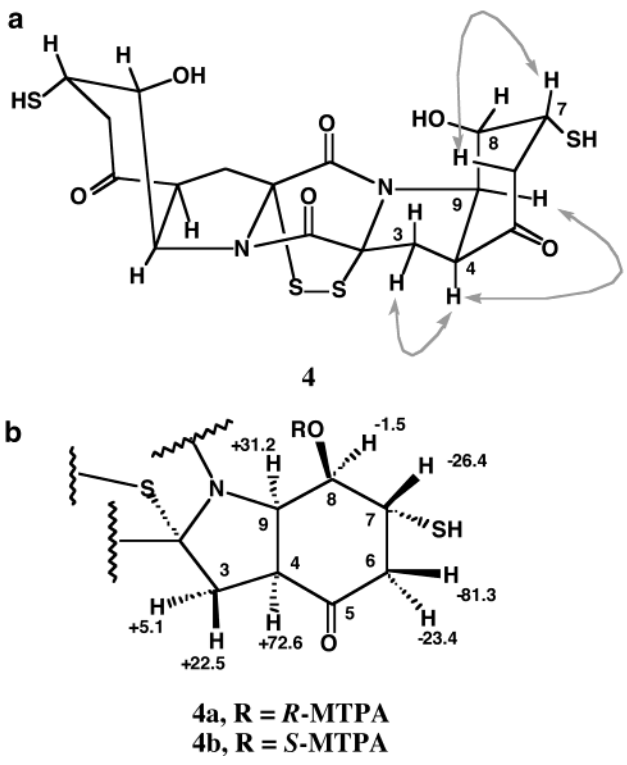

Figure 4. Relative and absolute stereochemistry of rostratin D (**4**): (a) arrows indicate critical NOE correlations used to establish relative stereochemistry and (b) $\Delta\delta$ values ($\delta_S - \delta_R$) in hertz for the two MTPA esters **4a** and **4b**.

507 in the positive mode, while $[M - H]^-$ and $[M + {}^{35}Cl]^-$ ions were displayed at *m/z* 483 and 519 in the negative mode, indicating the molecular weight of **3** was 484. High-resolution MALDI mass spectral data showed an intense fragment ion at *m/z* 443.1444 ($[C_{20}H_{24}N_2O_8 + Na]^+$ requires 443.1431) and 421.1622 ($[C_{20}H_{24}N_2O_8 + H]^+$ requires 421.1611), which, as in the cases of **1** and **2**, were fragment ions produced by loss of S_2 from the corresponding $[M + Na]^+$ and $[M + H]^+$ ions. Accordingly, the molecular formula of **3** could be defined as $C_{20}H_{24}N_2O_8S_2$. Analysis of ^1H NMR data (Table 3) showed that many of the structural features of **2** were intact in **3**. The presence of two additional methoxyl functionalities in **3** was recognized by the sharp 6H singlet at δ 3.21. As in rostratins A and B, **3** showed symmetrical NMR features with only half of the carbon and proton signals being observed. Comprehensive analysis of 2D NMR data allowed all protons and carbons to be assigned. It was again clear that rostratin C possessed a cyclohexane ring and the same bicyclic diketopiperazine disulfide as in rostratins A and B. COSY NMR data, which again defined the spin system from C-6(6′)−C-9(9′) and C-9(9′) to C-3(3′), allowed the location of the methoxyl group to be placed at C-7(7′). The coupling constant data for the C-7(7′) to C-9(9′) proton array showed the presence of a chair cyclohexane ring and allowed the methoxyl and hydroxyl functionalities to be assigned to equatorial and axial positions, respectively. The methoxyl methyl group, as anticipated, was a useful marker for the HMBC experiment [HMBC correlations with C-7(7′)], confirming its location at that carbon.

The relative stereochemistry for **3** was determined by NOE difference spectroscopy and by a 2D NOESY experiment, which confirmed the C-4(4′)−C-9(9′) ring juncture as *cis* and the stereochemistries of all substituents on the cyclohexane rings. As in **2**, H-4(4′) showed NOESY correlations with H-9(9′) and H-3α(3′α). Proton H-9(9′) showed correlations with H-8(8′), while the methoxyl group methyl

Table 3. NMR Spectral Assignments for **3** in DMSO-d_6

C#	δ_C	δ_H (m, *J* in Hz)	COSY	HMBC
1/1′	161.8, C			3/3′(β)
2/2′	76.2, C			3/3′(β), 4/4′, 9/9′
3/3′	32.6, CH2	(α) 2.69 (dd, 14.4, 1.6)	3/3′(β), 4/4′	4/4′
		(β) 2.99 (dd, 14.4, 8.0)	3/3′(α), 4/4′	
4/4′	46.4, CH	3.20 (br dd, 8.0, 7.2)	3/3′, 9/9′	
5/5′	207.4, C			9/9′, 7/7′, 3/3′(β)
6/6′	40.7, CH2	(α) 2.61 (dd, 16.4, 4.8)	6/6′(β), 7/7′	8/8′
		(β) 2.72 (dd, 16.4, 10.4)	6/6′(α), 7/7′	
7/7′	75.5, CH	3.28 (ddd, 10.4, 4.8, 1.6)	6/6′	OH, 8/8′, 9/9′, OMe
8/8′	61.8, CH	5.01 (m)	6/6′, 9/9′, OH	6/6′, 9/9′, OH
9/9′	63.2, CH	4.40 (dd, 7.2, 4.4)	4/4′, 8/8′	3/3′(α), 4/4′, 8/8′, OH
OMe	56.0, CH3	3.21 s		7/7′
OH		5.63 (d, 4.8)	8/8′	

Table 4. NMR Spectral Assignments for **4** in DMSO-d_6

C#	δ_C	δ_H (m, *J* in Hz)	COSY	HMBC
1/1′	162.5, C			3/3′(β), 9/9′
2/2′	73.6, C			3/3′, 4/4′, 9/9′
3/3′	45.9, CH2	(α) 2.55 (br d, 12.8)	3/3′(β), 4/4′	4/4′, 9/9′
		(β) 2.85 (dd, 12.8, 8.4)	3/3′(α), 4/4′	
4/4′	43.2, CH	3.27 (br dd, 8.4, 7.5)	3/3′, 9/9′	3/3′, 8/8′, 9/9′
5/5′	207.4, C			3/3′, 7/7′, 9/9′
6/6′	38.0, CH2	(α) 2.43 (br d, 18.8)	6/6′(β), 7/7′	4/4′, 8/8′
		(β) 3.07 (dd, 18.8, 6.0)	6/6′(α), 7/7′	
7/7′	45.2, CH	3.71 (m)	6/6′, 8/8′	6/6′, 9/9′, OH
8/8′	65.2, CH	4.47 (m)	6/6′(β), 9/9′, OH	6/6′(α), 7/7′, 9/9′
9/9′	61.8, CH	4.46 (br dd, 7.5, 2.1)	4/4′, 8/8′	3/3′(α), 4/4′, 7/7′, OH
OH		6.06 (d, 3.6)	8/8′	
SH		3.34 (s)		

showed a correlation with the C-8(8′) hydroxyl group proton (Figure 3). The combined NOE measurements showed that rostratin C has the same overall configuration as in **2** and that the methoxyl at C-7(7′) is equatorial while the hydroxyl at C-8(8′) is in an axial position.

Using the identical modified Mosher methods, the absolute stereochemistry of **3** was readily defined by analysis of NMR shift data from the corresponding C-8(8′) (*R*)- and (*S*)-MTPA bis-esters. The significant proton chemical shift differences between the (*R*)- and (*S*)-MTPA esters **3a** and **3b** demonstrated that C-8(8′) possesses the *R*-configuration (Figure 3).[26] These absolute stereochemical refinements required that rostratin C (**3**) possess C-4(4′) = *S*, C-7(7′) = *S*, and C-9(9′) = *R* absolute configurations.

Rostratin D (**4**) was obtained as a colorless gum, which showed strong IR absorptions at 3356 (OH), 1698 (ketone), and 1662 (amide) cm^{-1}. The high-resolution MALDI mass spectrum of **4** showed a protonated molecular ion at *m*/*z* 489.0261, demonstrating that the molecular formula of rostratin D was $C_{18}H_{20}N_2O_6S_4$ ($[C_{18}H_{20}N_2O_6S_4 + H]^+$ requires 489.0283). This formula incorporates two additional sulfur atoms in comparison to the formula of rostratin B and, to maintain the appropriate degrees of unsaturation, indicates the presence of two thiol functionalities. Comprehensive analysis of combined NMR data showed that **4** was a close relative of rostratin C (**3**) and possessed the symmetry characteristics of this class of disulfide with only half of the NMR bands being observed (Table 4). Again, COSY data and spin decoupling experiments showed the same spin system as in **3**, which established the connectivity through C-6(6′), C-7(7′), C-8(8′), C-9(9′), C-4(4′), and C-3(3′). These data demonstrated the presence of a hydroxyl functional group at C-8(8′) and, on the basis of chemical shift data (δ_C = 45.2, δ_H = 3.71 m), showed that the thiols were positioned at C-7(7′). Furthermore, analysis of the coupling constant data for the substituted cyclohexane ring indicated that the C-7(7′) thiols and the C-8(8′) hydroxyl groups were in axial positions. The coupling constants of H-7(7′), although observed as a complex multiplet, were readily deciphered from the adjacent methylene proton coupling constants at C-6(6′). Besides a large geminal coupling, one of the C-6(6′) protons showed a 6 Hz coupling to H-7(7′), while the other proton was not coupled. This indicated the lack of an axial proton at C-7(7′). Likewise, the small coupling constants observed (2.1 Hz) from H-9(9′) to H-8(8′) showed that these protons were also in equatorial positions.

The relative stereochemistry for **4** was confirmed by NOE difference spectroscopy and interpretation of 2D NOESY data. As in **2** and **3**, correlations between H-4(4′), H-9(9′), and H-3α(3′α) showed the *cis* relationship of the C-4(4′)−C-9(9′) ring juncture and strongly inferred that the disulfide bridge was α-oriented in a fashion identical to the other metabolites. While the axial orientation of the thiols at C-7(7′) were strongly indicated by coupling constant data, it was confirmed by NOE experiments. A strong NOE correlation was observed from H-6β(6′β) to the adjacent H-7(7′) proton, indicating the latter was in the equatorial position. NOE correlations between H-8(8′) and H-9(9′) were not observed because these two signals overlapped.

The absolute stereochemistry of rostratin D (**4**) was also assigned by interpretation of chemical shift data derived from the corresponding C-8(8′) (*R*)- and (*S*)-MTPA esters. Using the selective Mosher's acylation described above for rostratin A (**1**), only the (*R*)- and (*S*)-MTPA O-bis-esters at C-8(8′) were produced.[27] This was accomplished by maintaining the NMR-tube reaction at 23 °C for 1.2 h. Here too, significant chemical shift differences between the (*R*)- and (*S*)-MTPA esters **4a** and **4b** defined C-8(8′) as *R* (Figure 4).[28] Considering the relative stereochemistry defined for all chiral centers allowed assignment of C-4(4′) = *S*, C-7(7′) = *R*, and C-9(9′) = *R* configurations.

Rostratins A−D (**1**−**4**) are a series of highly C_2-symmetrical diketopiperazine disulfides that possess an obvious relationship with exserohilone, a metabolite also found in this mixture.[28] It is curious that the rostratins are C-2(2′)

disulfides and exserohilones the corresponding C-2(2′)-bis methyl sulfides. Whether this change has an affect on the biological activities of the rostratins is unclear. Another significant issue within this class of metabolites is the different stereochemistry of the C-4(4′)−C-9(9′) ring juncture in **1** as opposed to **2**−**4**, with rostratin A being *trans* and rostratins B−D *cis* ring fused. This seemed unusual, but confident NOE and vicinal coupling constant data clearly showed this difference. Rostratins A−D showed diverse in vitro cytotoxicities against HCT-116 human colon carcinoma with IC_{50} values of 8.5, 1.9, 0.76, and 16.5 μg/mL (9, 4.4, 1.6, and 35 μM), respectively. The significant spread in these numbers, in particular the increased potency of **2** and **3**, suggests that the C-5(5′) ketone functionality may be a contributing factor. The greatly reduced cytotoxicity of **4**, however, argues against this simplistic analysis.

The development of the selective Mosher acylation method reported here, using temperature-controlled, in-NMR-tube acylation, afforded single (bis) MTPA esters of **1** and **4** in excellent yields. This method, which allows for in-NMR-tube reactions and subsequent data acquisition, provides an attractive new technique to generate absolute stereochemical information for polyfunctional molecules. We demonstrated that this method can be utilized using very simple temperature control methods (salt/ice baths), but point out that this procedure could be very highly refined, perhaps generating much more selectivity control, by utilization of NMR low-temperature probes.

Experimental Section

General Experimental Procedures. The optical rotations were measured on a Rudolph Research Autopol III polarimeter with a path length of 10 cm at the sodium D line (589 nm). UV spectra were obtained on a Beckman Coulter DU 640. The IR spectrum was recorded on a Perkin-Elmer 1600 FTIR instrument as a film on a NaCl disk. ^{1}H and ^{13}C NMR spectra were obtained in DMSO-d_6 on a Varian Inova Instrument at 400 and 100 MHz, respectively, while all 2D NMR experiments were performed at 300 MHz on an Inova spectrometer. Chemical shifts are expressed in δ (ppm) using the residual NMR solvent signals as internal standard. Low-resolution mass spectra were obtained on a Hewlett-Packard MSD 1100 LC-MS system. HPLC separations were conducted with a Rainin DYNAMAX-60 Å ODS column (250 × 10 mm) at a flow rate of 2.5 mL/min utilizing refractive index detection.

Fungus Source and Cultivation. Strain CNK-630 was isolated from a cyanobacterial mat collected off the northwest corner of Lanai Island, Hawaii, in 1997. The mat sample was air-dried at room temperature overnight in a laminar flow hood, and the dried material was directly plated onto SSE agar [2 g of soluble seaweed (*Ascophyllum nodosum*), 16 g of agar, 1 L of seawater, penicillin G/streptomycin sulfate 150 μg/mL]. Fungal hyphae observed growing away from the cyanobacterial mat were transferred to new media until a pure culture was obtained. Strain CNK-630 was identified as *Exserohilum rostratum* (Drechsler) Leonard & Suggs, on the basis of morphological features, by the Centraalbureau voor Schimmelcultures (www.cbs.knaw.nl), The Netherlands. This strain is available from the Marine Microorganism Collection at the Scripps Institution of Oceanography.

E. rostratum, our strain CNK-630, was cultivated without shaking for 26 days at room temperature in 20 × 1 L volumes using culture medium CK1 (5 g of mannitol, 4 mL of 50% fish solubles, 2 g of menhaden meal, 2 g of kelp powder, 1 L of seawater). The whole culture was extracted twice with ethyl acetate, the organic phase was separated and dried with anhydrous sodium sulfate, and the solvent was removed under vacuum.

Extraction and Isolation. The methanol-soluble component of the whole culture extract (4.5 g from 20 L) was subjected to C-18 reversed-phase flash chromatography eluting with a gradient of H_2O and MeOH. More than 70 × 20 mL fractions were collected; they were then analyzed by normal-phase silica TLC and consequently combined on the basis of homogeneity into five superfractions (A: 1426.3 mg, B: 216.2 mg, C: 196.3 mg, D: 313.7 mg, and E: 1571.8 mg). Superfractions B−D showed significant cytotoxicity and were subsequently independently fractionated using HCT-116 cytotoxicity as a guide. Fractionation of superfraction B by Sephadex LH-20 column chromatography (MeOH) gave three fractions (B-1: 89.8 mg, B-2: 22.5 mg, and B-3: 114.4 mg). Fraction B-1 contained a mixture of pigments and exserohilone (**5**). Sephadex LH-20 fractionation of fraction C (MeOH) gave fractions C-1 (33.4 mg), C-2 (23.9 mg), C-3 (46.5 mg), C-4 (31.7 mg), and C-5 (18.5 mg). Fraction C-3, which showed the majority of the cytotoxicity, was subjected to repeated Sephadex LH-20 separation (MeOH) to yield rostratin A (**1**) (11.2 mg, 0.56 mg/mL). Fraction D was further fractionated by C-18 reversed-phase column chromatography, eluting with a H_2O/MeCN gradient, to afford four complex fractions (D-1: 23.8 mg, D-2: 28.5 mg, D-3: 14.7 mg, D-4: 18.2 mg, and D-5: 48.0 mg), of which D-3 and D-4 showed significant cytotoxicity. Repeated chromatography of D-3 and D-4 using Sephadex LH-20 with mixtures of $CHCl_3$/MeOH (2:3, 1:1, and 2:1) afforded rostratin C (**3**) (8.2 mg, 0.41 mg/L), rostratin B (**2**) (6.2 mg, 0.31 mg/L), and rostratin D (**4**) (5.2 mg, 0.26 mg/L).

Rostratin A (1): colorless gum; $[\alpha]^{20}_D$ −185° (*c* 0.0037, MeOH/CH_2Cl_2, 1:1); IR ν_{max} 3331 (OH), 1666 (amide) cm^{-1}; ^{1}H NMR, ^{13}C NMR, ^{1}H−^{1}H COSY, and HMBC, see Table 1; ESIMS (positive mode) *m/z* 429 $[M + H]^+$; ESIMS (negative mode) *m/z* 463 $[M + {}^{35}Cl]^-$; HR-MALDI-MS *m/z* 365.1723 (calcd for $[C_{18}H_{24}N_2O_6 + H]^+$ 365.1713).

Rostratin B (2): colorless gum; $[\alpha]^{20}_D$ −210° (*c* 0.0004, MeOH/CH_2Cl_2, 1:1); IR ν_{max} 3413 (br, OH), 1705 (ketone), and 1666 (amide) cm^{-1}; ^{1}H NMR, ^{13}C NMR, ^{1}H−^{1}H COSY, and HMBC, see Table 2; API-ES MS (negative mode) *m/z* 423 $[M - H]^-$; ESIMS *m/z* 459 $[M + {}^{35}Cl]^-$; HR-MALDI-MS *m/z* 361.1387 (calcd for $[C_{18}H_{20}N_2O_6 + H]^+$ 361.1400).

Rostratin C (3): colorless gum; $[\alpha]^{20}_D$ −167° (*c* 0.0022, MeOH/CH_2Cl_2, 1:1); IR ν_{max} 3395 (br OH), 1703 (ketone), and 1673 (amide) cm^{-1}; ^{1}H NMR, ^{13}C NMR, ^{1}H−^{1}H COSY, and HMBC, see Table 3; ESIMS (positive mode) *m/z* 507 ($[M + Na]^+$); ESIMS (negative mode) *m/z* 483 ($[M - H]^-$) and 519 ($[M + {}^{35}Cl]^-$); HR-MALDI-MS *m/z* 443.1444 (calcd for $[C_{20}H_{24}N_2O_8 + Na]^+$ 443.1431).

Rostratin D (4): colorless gum; $[\alpha]^{20}_D$ +108° (*c* 0.0069, MeOH/CH_2Cl_2, 1:1); IR ν_{max} 3356 (OH), 1698 (ketone), and 1662 (amide) cm^{-1}; ^{1}H NMR, ^{13}C NMR, ^{1}H−^{1}H COSY, and HMBC, see Table 4; HR-MALDI-MS *m/z* 489.0261 (calcd for $[C_{18}H_{20}N_2O_6S_4 + H]^+$ 489.0283).

Lithium Aluminum Hydride Reduction of Rostratin A (1) to the Amino Alcohol (6). While stirring at −5 °C, $LiAlH_4$ (2.8 mg, 74 μmol) was added stepwise to a solution of **1** (5 mg, 11.7 μmol) in THF (1.2 mL) over a 20 min period. The reaction mixture was refluxed for 5 h before it was quenched with ice (~1 g), the precipitate was dissolved by adding 10 drops of 10% H_2SO_4, and the pH was adjusted to 8.5 ± 0.5 with 10% K_2CO_3. The whole mixture was reduced to dryness under vacuum and exhaustively extracted with CH_2Cl_2/MeOH (1:1). Removal of the extraction solvent under vacuum gave a residual material that was fractionated by silica gel column chromatography (10 × 50 mm), eluting with CH_2Cl_2/MeOH (10:1), to yield the desired amino alcohol **6** (0.5 mg, 9.8% yield): API-ES MS (negative mode) *m/z* 218 $[M - H]^-$, 200 $[M - H - H_2O]^-$; ^{1}H NMR (400 MHz, CD_3OD, assigned by its COSY and NOESY spectra) δ 3.72 (s, 2H, H-1), 2.01 (m, 1H, H-3), 1.39 (dd, 1H, J = 13.2, 5.1 Hz, H-3), 1.71 (m, 1H, H-4), 3.60 (m, 2H, H-5 and H-8), 1.62 (m, 2H, H-6α and H-7α), 1.98 (m, 2H, H-6β and H-7β), 3.68 (t, 1H, J = 6.3 Hz, H-9).

Procedure for the in-NMR-Tube Selective Mosher's Reaction to Produce Mono-MTPA Esters. (1) The sample is dissolved in pyridine-d_5 in an NMR tube dried under a gentle nitrogen stream. (2) A ^{1}H NMR spectrum is recorded as a reference. (3) The NMR tube is precooled to −4 °C or below

using a salt−ice bath, and a carefully calculated amount of MTPA chloride is added. (4) The NMR tube is rigorously shaken until the liquids are evenly mixed. (5) The NMR tube is inserted into a small beaker of ice water, which is then allowed to warm at a rate of 1 deg every 5 min. (6) The ^{1}H NMR spectrum is recorded every 30 min. (7) When evidence of acylation is observed, the NMR tube is maintained at that temperature until complete conversion has been observed. (8) The acylation reaction is then quenched by cooling the NMR tube in an ice−water bath and adding one drop of D_2O (to hydrolyze excess MTPA chloride). (9) The ^{1}H NMR COSY and/or NOESY spectra are then acquired to derive ^{1}H NMR data of the MTPA esters, resolving the overlapping MTPA product signals when necessary. It should be emphasized that this procedure is a general guide for selective MTPA acylation, as other important factors such as the molar ratio of sample and MTPA chloride, moisture in pyridine-d_5, and the purity of MTPA chloride can also have a negative effect on the reaction.

Preparation of (*S*)- and (*R*)-MTPA Esters (1a and 1b) from Rostratin A (1). Following the procedure summarized above, compound **1** (1.8 mg, 4.2 μmol) was acylated in an NMR tube with (*S*)-MTPA chloride (2.0 μL, 10.6 μmol) in pyridine-d_5. The selective acylation was achieved at 28 °C for 3 h, with compound **1** being transformed entirely into the desired (*R*)-MTPA ester **1a**: ^{1}H NMR (300 MHz, pyridine-d_5, assigned by its COSY and NOESY spectra) δ 3.356 (dd, 1H, J = 10.2, 3.3 Hz, H-3), 3.097 (t, 1H, J = 10.2 Hz, H-3), 2.660 (dddd, 1H, J = 10.8, 8.7, 8.1, 3.3 Hz, H-4), 5.319 (ddd, 1H, J = 8.1, 7.2, 3.3 Hz, H-5), 1.570 (m, 1H, H-6α), 2.218 (m, 1H, H-6 β), 2.195 (m, 1H, H-7α), 1.570 (m, 1H, H-7β), 3.909 (ddd, 1H, J = 8.7, 7.4, 3.3 Hz, H-8), 3.650 (dd, 1H, J = 10.8, 8.7 Hz, H-9). In the same fashion, compound **1** was treated with (*R*)-MTPA chloride in pyridine-d_5 to give the expected (*S*)-MTPA ester **1b**: ^{1}H NMR (300 MHz, pyridine-d_5, assigned by its COSY and NOESY spectra) δ 3.738 (dd, 1H, J = 10.5, 3.3 Hz, H-3), 3.274 (t, 1H, J = 10.5 Hz, H-3), 2.747 (dddd, 1H, J = 10.2, 8.7, 8.1, 3.3 Hz, H-4), 5.318 (ddd, 1H, J = 8.1, 7.4, 3.3 Hz, H-5), 1.433 (m, 1H, H-6α), 2.211 (m, 1H, H-6β), 2.184 (m, 1H, H-7α), 1.554 (m, 1H, H-7β), 3.893 (ddd, 1H, J = 8.1, 7.4, 3.3 Hz, H-8), 3.716 (t, 1H, J = 8.1 Hz, H-9); ^{1}H NMR (300 MHz, pyridine-d_5, assigned by spin decoupling) of **1**, as a reference spectrum for the selective Mosher's reaction, δ 3.023 (m, 2H, H-3α and H-3β), 2.568 (m, 1H, H-4), 3.821 (m, 1H, H-5), 2.163 (m, 2H, H-6β and H-7α), 1.565 (m, 2H, H-6α and H-7β), 3.91 (m, 1H, H-8), 3.450 (dd, 1H, J = 11.4, 9.0 Hz, H-9).

Preparation of (*R*)- and (*S*)-MTPA Esters (2a and 2b) of Rostratin B (2). After dissolving in pyridine-d_5 (0.5 mL) under a gentle N_2 stream, compound **2** (1.5 mg, 3.5 μmol) was placed in a dried, clean NMR tube, and (*S*)-MTPA chloride (2.0 μL, 10.6 μmol) was added and immediately shaken until uniformly mixed. After sealing with Parafilm, the NMR tube was kept overnight at room temperature. The ^{1}H NMR spectrum, recorded directly from the reaction NMR tube, showed the production of the corresponding (*R*)-MTPA ester **2a**: ^{1}H NMR (300 MHz, pyridine-d_5, assigned by its COSY and NOESY spectra) δ 3.283 (dd, 1H, J = 13.6, 8.6 Hz, H-3β), 3.270 (dd, 1H, J = 13.6, 1.6 Hz, H-3α), 3.234 (ddd, 1H, J = 8.6, 7.6, 1.6 Hz, H-4), 2.640 (m, 1H, H-6α), 2.625 (m, 1H, H-6β), 2.097 (m, 1H, H-7α), 2.291 (m, 1H, H-7β), 6.868 (m, 1H, H-8), 4.817 (dd, 1H, J = 7.6, 3.6 Hz, H-9). In an identical fashion, compound **2**, (*R*)-MTPA chloride, and pyridine-d_5 were combined in an NMR tube and allowed to stand overnight. ^{1}H NMR measurements showed the quantitative conversion of **2** to the anticipated (*S*)-MTPA ester **2b**: ^{1}H NMR (300 MHz, pyridine-d_5, assigned by its COSY and NOESY spectra) δ 3.365 (dd, 1H, J = 12.4, 7.2 Hz, H-3β), 3.310 (dd, 1H, J = 12.4, 1.6 Hz, H-3α), 3.475 (ddd, 1H, J = 8.4, 7.2, 1.6 Hz, H-4), 2.538 (m, 1H, H-6α), 2.465 (m, 1H, H-6β), 2.070 (m, 1H, H-7α), 2.205 (m, 1H, H-7β), 6.838 (m, 1H, H-8), 4.947 (dd, 1H, J = 8.4, 3.6 Hz, H-9).

Preparation of (*R*)- and (*S*)-MTPA Esters (3a and 3b) of Rostratin C (3). Compound **3** (2.5 mg, 5.2 μmol) was treated in a dried, clean NMR tube with (*S*)-MTPA chloride (2.2 μL, 11.6 μmol) following the procedure for the Mosher reaction of compound **2** to give the corresponding (*R*)-MTPA ester **3a**: ^{1}H NMR (300 MHz, pyridine-d_5, assigned by its COSY and NOESY spectra) δ 3.379 (dd, 1H, J = 13.5, 5.4 Hz, H-3α), 3.291 (br d, 1H, J = 13.5 Hz, H-3β), 3.238 (br dd, 1H, J = 7.6, 7.0 Hz, H-4), 3.141 (dd, 1H, J = 16.0, 4.4 Hz, H-6α), 2.926 (dd, 1H, J = 16.0, 10.4 Hz, H-6β), 3.877 (ddd, 1H, J = 11.6, 4.1, 3.6 Hz, H-7), 5.233 (m, 1H, H-8), 4.899 (dd, 1H, J = 7.6, 6.4 Hz, H-9), 3.392 (s, 3H, OCH_3). Treatment of **3** in the same manner with (*R*)-MTPA chloride in pyridine-d_5 showed a quantitative conversion into the (*S*)-MTPA ester **3b**: ^{1}H NMR (300 MHz, pyridine-d_5, assigned by its COSY and NOESY spectra) δ 3.401 (dd, 1H, J = 14.1, 3.6 Hz, H-3α), 3.344 (br d, 1H, J = 14.1 Hz, H-3β), 3.544 (br dd, 1H, J = 8.3, 7.4 Hz, H-4), 3.091 (dd, 1H, J = 16.8, 4.4 Hz, H-6α), 2.801 (dd, 1H, J = 16.8, 10.5 Hz, H-6β), 3.848 (ddd, 1H, J = 10.4, 6.0, 2.4 Hz, H-7), 5.173 (m, 1H, H-8), 5.149 (t, 1H, J = 6.4 Hz, H-9), 3.288 (s, 3H, OCH_3).

Preparation of (*R*)- and (*S*)-MTPA Esters (4a and 4b) of Rostratin D (4). Compound **4** (2.7 mg, 5.5 μmol) was acylated in an NMR tube by the selective Mosher's method with (*S*)-MTPA chloride (2.5 μL, 13.3 μmol, an excess quantity of (*S*)-MTPA chloride was used due to the presence of MeOH in the sample and the moisture in pyridine-d_5). The desired selective acylation occurred at 23 °C, and this temperature was maintained for 1.2 h to give the (*R*)-MTPA ester **4a**: ^{1}H NMR (300 MHz, pyridine-d_5, assigned by its COSY and NOESY spectra) δ 3.423 (dd, 1H, J = 10.2, 6.3 Hz, H-3α), 3.184 (br d, 1H, J = 10.4 Hz, H-3β), 3.246 (dd, 1H, J = 6.6, 6.3 Hz, H-4), 2.886 (br d, 1H, J = 18.9 Hz, H-6α), 3.085 (dd, 1H, J = 18.9, 5.4 Hz, H-6β), 4.299 (m, 1H, H-7), 6.507 (t, 1H, J = 2.4 Hz, H-8), 5.199 (br d, 1H, J = 6.6 Hz, H-9). Treatment of **4**, in an identical fashion with (*R*)-MTPA chloride in pyridine-d_5, gave the expected (*S*)-MTPA ester **4b**: ^{1}H NMR (300 MHz, pyridine-d_5, assigned by its COSY and NOESY spectra) δ 3.440 (dd, 1H, J = 10.2, 6.3 Hz, H-3α), 3.259 (br d, 1H, J = 11.7 Hz, H-3β), 3.488 (dd, 1H, J = 6.6, 6.3 Hz, H-4), 2.808 (m, 2H, H-6α and H-6β), 4.211 (m, 1H, H-7), 6.502 (t, 1H, J = 2.4 Hz, H-8), 5.303 (br d, 1H, J = 6.6 Hz, H-9); ^{1}H NMR (300 MHz, pyridine-d_5, assigned by spin decoupling) of **4** (as reference spectrum for the selective Mosher's acylation procedure) δ 3.000 (dd, 1H, J = 10.2, 6.6 Hz, H-3β), 3.278 (br d, 1H, J = 10.2 Hz, H-3α), 2.465 (dd, 1H, J = 6.6, 6.3 Hz, H-4), 3.597 (dd, 1H, J = 14.4, 4.8 Hz, H-6β), 2.843 (br d, 1H, J = 14.4 Hz, H-6α), 3.914 (ddd, 1H, J = 4.8, 3.2, 1.5 Hz, H-7), 5.280 (dd, 1H, J = 3.2, 2.0 Hz, H-8), 5.117 (ddd, 1H, J = 6.3, 2.0, 1.2 Hz, H-9).

Acknowledgment. This research is a result of financial support from the National Institutes of Health, National Cancer Institute under grant CA 67775. R.X.T. acknowledges The Hwa-Ying Education and Culture Foundation for providing a sabbatical fellowship. We thank C. Kauffman for his assistance in the microbiological aspects of this project.

Supporting Information Available: ^{1}H NMR spectra of (*R*)- and (*S*)-MTPA derivatives of **1**, ^{1}H NMR spectrum of **1** in pyridine-d_5, and NOE difference and COSY spectra of **1b**. This material is available free of charge via the Internet at http://pubs.acs.org.

References and Notes

(1) Nygren, P.; Larsson, R. *J. Internal Med.* **2003**, *253*, 46−75, and related references therein.
(2) Fusetani, N. *Drugs from the Sea*; Karger: Basel, 2000.
(3) Fenical, W. *Chem. Rev.* **1993**, *93*, 1673−1683.
(4) Mincer, T. J.; Jensen, P. R.; Kauffman, C. A.; Fenical, W. *Appl. Environ. Microbiol.* **2002**, *68*, 5005−5011.
(5) Feling, R. H.; Buchanan, G. O.; Mincer, T. J.; Kauffman, C. A.; Jensen, P. R.; Fenical, W. *Angew. Chem., Int. Ed.* **2003**, *42*, 355−357.
(6) Cueto, M.; Jensen, P. R.; Fenical, W. *Org. Lett.* **2002**, *4*, 1583−1585.
(7) Renner, M. K.; Jensen, P. R.; Fenical, W. *J. Org. Chem.* **2000**, *65*, 4843−4852.
(8) De, R.; Purkait, R.; Pal, A. K.; Purkayastha, R. P. *Indian J. Exp. Biol.* **1999**, *37*, 706−709.
(9) Chandramohan, S.; Charudattan, R. *Biol. Control* **2001**, *22*, 246−255.
(10) Alker, A. P.; Smith, G. W.; Kim, K. *Hydrobiologia* **2001**, *460*, 105−111.
(11) The HCT-116 growth inhibition assay was conducted in accord with: Lee, F. Y.; Borzilleri, R.; Fairchild, C. R.; Kim, S.-H.; Long, B. H.; Reventos-Suarez, C.; Vite, G. D.; Rose, W. C.; Kramer, R. A. *Clin. Cancer Res.* **2001**, *7*, 1429−1437.

(12) Sugawara, K.; Sugawara, M.; Strobel, G. A.; Fu, Y.; Cun-Heng, H.; Clardy, J. *J. Org. Chem*. **1985**, *50*, 5631−5633.
(13) Kwon, O. S.; Park, S. H.; Yun, B. S.; Pyun, Y. R.; Kim, C.-J. *J. Antibiot.* **2001**, *54*, 179−181.
(14) Jayatilake, G. S.; Thornton, M. P.; Leonard, A. C.; Grimwade, J. E.; Baker, B. J. *J. Nat. Prod.* **1996**, *59*, 293−296.
(15) Harada, N.; Nakanishi, K. *Circular Dichroic Spectroscopy−Exciton Coupling in Organic Stereochemistry*; University Science Books: Mill Valley, CA, 1983.
(16) Dale, J. A.; Dull, D. L.; Mosher, H. S. *J. Org. Chem*. **1969**, *34*, 2543−2549.
(17) Ohtani, I.; Kusumi, T.; Kashman, Y.; Kakisawa, H. *J. Am. Chem. Soc.* **1991**, *113*, 4092−4096.
(18) Guilet, D.; Guntern, A.; Ioset, J.-R.; Queiroz, E. F.; Ndjoko, K.; Foggin, C. M.; Hostettman, K. *J. Nat. Prod.* **2003**, *66*, 17−20.
(19) Su, B.-N.; Park, E. J.; Mbwambo, Z. H.; Santarsiero, B. D.; Mesecar, A. D.; Fong, H. H. S.; Pezzuto, J. M.; Kinghorn, A. D. *J. Nat. Prod.* **2002**, *65*, 1278−1282.
(20) Seco, J. M.; Quiñoa, E.; Riguera, R. *Tetrahedron Asymmetry* **2000**, *11*, 2781−2791.
(21) Seco, J. M.; Martino, M.; Quiñoa, E.; Riguera, R. *Org. Lett.* **2000**, *2*, 3261−3264.
(22) MacMillian, J. B.; Molinski, T. *Org. Lett.* **2002**, *4*, 1535−1538.
(23) Konno, K.; Fujishima, T.; Liu, Z.-P.; Takayama, H. *Chirality* **2002**, *14*, 72−80.
(24) The difference in the rates of acylation of the hydroxyl groups on C-5(5′) and C-8(8′) in **1** is likely due to the ability of the latter to form a hydrogen bond to the carbonyl on C-1(1′). Inspection of molecular models suggests these two functional groups are quite close.
(25) For an example of the reduction of amides to alcohols by $LiAlH_4$, see: Birkofer, L.; Frankus, E. *Ber.* **1961**, *94*, 216.
(26) It should be noted that **3** is assigned a C-8(8′) = *R* configuration, while **1** and **2** possess C-8(8′) = *S* configurations despite the fact that the hydroxyl groups are alpha in all three metabolites. The replacement of one of the hydrogens at C-8(8′) in **1** and **2** with a methoxyl functionality in **3** reverses the Cahn−Ingold−Prelog priorities. The same phenomenon is seen with rostratin D (**4**).
(27) The regioselective acylation of **4** is most likely due to the greater nucleophilicity of the alcohol as compared to the thiol.
(28) Other structurally related compounds include the following. (a) Epicorazines A−C: Kleinwachter, P.; Dahse, H.-M.; Luhmann, U.; Schlegel, B.; Dornberger, K. *J. Antibiot.* **2001**, *54*, 521−525, and references therein. (b) Epoxyexserohilone: Cutler, H. G.; Hoogsteen, K.; Littrell, R. H.; Arison, B. H. *Agric. Biol. Chem*. **1991**, *55*, 2037−2042. We thank the reviewer who brought the latter example to our attention.

NP049920B